Dalton Transactions

Accepted Manuscript

ROYAL SOCIETY OF CHEMISTRY

www.rsc.org/dalton

Journal Name

ARTICLE

An effective approach for modifying carbonaceous materials with niobium single sites to improve their catalytic properties

Received 00th January 20xx,
Accepted 00th January 20xx

DOI: 10.1039/x0xx00000x

www.rsc.org/

A. S. Bozzi[a], R. L. Lavall[a], T. E. Souza[a], M. C. Pereira[b], P. P. de Souza[c], H. A. De Abreu[a], A. De Oliveira[a], P. F. R. Ortega[a], R. Paniago[d], L. C. A. Oliveira[a]†

In this paper we show a very simple route for the incorporation of catalytically active niobium species on the surface of carbon materials, such as graphene oxide, carbon nanotubes and activated carbon. Some existing methods of incorporating transition metal on a support have involved the co-precipitation or wet impregnation, to obtain the corresponding oxides. These methods, however, cause a reduction in specific area of the support and also can form large metal oxide particles with loss of metal exposure. Therefore, here we present a novel way to add catalytically active species on the surface of different types of carbon through the formation of interaction complexes between the metal precursor and the functional groups of the carbon matrix. Because of the excellent catalytic properties exhibited by niobium species we choose the NH4[NbO(C2O4)2(H2O)2].2H2O salt as a model precursor. The characterizations by XPS reveal the presence of the niobium species indicated by the displacement of the peaks between 206-212 eV related to oxalate species according to the spectrum from pure niobium oxalate. Images obtained by TEM and SEM show typical morphologies of carbonaceous materials without the niobium oxide formation signal, which indicates the presence of niobium complexes as isolated sites on the carbon surfaces. This new class of material exhibited excellent properties as catalysts for pollutants oxidation. The presence of Nb promotes the catalytic activation of H_2O_2 generating hydroxyl radicals in situ, which allows their use in organic compound oxidation processes. Tests for DBT oxidation indicate that Nb significantly improves the removal of such pollutants in biphasic reactions with removal around 90% under the tested conditions. Theoretical calculations showed that the most favorable adsorption model is an ionic complex presenting a ΔG = -108.7 kcal mol^{-1} for the whole adsorption process.

Introduction

Carbon materials, such as graphene, carbon nanotubes (CNTs) and activated carbon (AC) have different technological applications ranging from development of electronic devices to adsorbent materials for removal of pollutants in water [1-5]. Particularly, the use of these materials in catalysis has become increasingly widespread among scientists worldwide. The high specific area and porosity present in these materials make them excellent catalysts or catalyst support [1-5]. When used as catalyst support, CNTs and graphene exhibit some unique advantages over the more traditional materials, such silica or alumina, because they not only have higher specific area, but they are also heat and electrical conductors and have extraordinary mechanical properties [6-11]. Moreover, compared to traditional carbon materials, in particular activated carbon, mass-transfer limitations during the reaction can be decreased, and therefore, the apparent activity and selectivity could be enhanced [12].

Different metals or metal oxides have been deposited on the surface of carbon materials by using several experimental methods, such as wet impregnation, sol-gel process, electro- and electrophoretic deposition, self-assembly processes and deposition from the gas phase, i.e. atomic layer deposition, chemical vapor deposition (CVD) and electron-beam evaporation [13]. Among these methods, the most common way to prepare supported active catalysts on the carbon surface is impregnation. However, when active catalytic species are deposited on a carbon support, there is a significant loss of its specific area, which directly affects the catalytic efficiency of the materials. Because of this, innovative approaches are needed to deposit active catalytic species on the carbon support without loss of specific area[1].

Here, we report a facile approach to attaching active catalytic species on a support without loss of surface area. The anionic diaquo niobate dioxalate (V) complex, derived from $NH_4[NbO(C_2O_4)_2(H_2O)_2].2H_2O$ salt, was bonded, under reflux

[a] Departament of Chemistry, Federal University of Minas Gerais, Av. Antonio Carlos 6627, Campus Pampulha, 31270-901, Belo Horizonte-MG, Brazil.
[b] Institute of Science, Engineering and Technology, Federal University of the Jequitinhonha and Mucuri Valleys, 39803-371, Téofilo Otoni- MG, Brazil .
[c] Departament of Chemisry, Federal Center Technological Education of Minas Gerais, CEFET-MG, Av. Amazonas 5243, 30421-169, Belo Horizonte-MG, Brazil..
[d] Departament of Physics, Federal University of Minas Gerais, Av. Antonio Carlos 6627, Campus Pampulha, 31270-901, Belo Horizonte-MG.
† E-mail: luizoliveira@qui.ufmg.br
Electronic Supplementary Information (ESI) available: [details of any supplementary information available should be included here]. See DOI: 10.1039/x0xx00000x

conditions, on three different types of carbon supports, i.e. activated carbon, functionalized nanotubes and graphene oxide, to show that our methodology can be applied to any carbon compound. The catalytic activity of the produced carbon materials was improved with the presence of diaquo niobate dioxalate (V) complex and was directly related to the interaction between the complex and the carbon support.

Experimental

Preparation of carbonaceous materials

The activated carbon was purchased from Sigma and used as received. A Nanocyl multiwalled carbon nanotube (MWCNT) with about 5 nm to 50 nm of diameter was treated with a concentrated acid mixture to add oxygenated groups to its surface. Briefly, 220 mg of MWCNT in a 240 mL of HNO_3:H_2SO_4 (1:3 v/v) solution was allowed to react in a low-frequency ultrasound bath for 3 h. The recovered solid was washed thoroughly with distilled water and dried overnight at 100 ^{o}C. This sample was named MWCNT-oxi. The amount of oxygenated groups attached to the surface (around 8%) was determined by thermogravimetry (Figure 1d) considering the weight loss between 120 ^{o}C and 400 ^{o}C. A few-layer graphene oxide (GO) was prepared by chemical exfoliation of expanded graphite flakes using a modified Hummers method [14].

Modification of carbon materials with niobium

A mass of ammonium niobium oxalate, ($NH_4[NbO(C_2O_4)_2(H_2O)](H_2O)n$) supplied by CBMM, Araxá – MG, Brazil, corresponding to 5 wt% of Nb was dissolved in 50 mL of distilled water and transferred to a 500 mL flask. About 1 g of the desired carbonaceous material (i.e. activated carbon, carbon nanotube or graphene) was suspended in 100 mL of distilled water using an ultrasound bath for 20 min. The suspension obtained was placed in the flask containing the niobium oxalate solution, and an additional volume of 200 mL of distilled water was added. The systems were putted in an ultrasound bath for 10 min, and then, refluxed for 6 h. After this period, the suspension was filtered under vacuum, and the recovered solid was washed thoroughly with distilled water. The modified carbonaceous material was dried at 80 °C for 3 h. For the grapheme oxide suspension, the filtration and washing steps were suppressed. The samples were named GO-Nb (Nb-containing graphene oxide), AC-Nb (Nb-containing activated carbon), and CNT-Nb (Nb-containing carbon nanotubes).

Material characterization

Thermogravimetric measurements were performed with a TGA Q5000 TA Instruments equipment at 5 ^{o}C min^{-1} under dry air flow of 100 mL min^{-1} from ambient temperature to 1000 ^{o}C. Scanning electron microscopy (SEM) was performed with a Scanning Electron Microscope with a cannon emission field effect Quanta 200 - FEG/FEI. The powder of the carbonaceous samples was placed on a carbon tape. Transmission electron microscopy (TEM) and EDS analysis were carried out with a Tecnai - G2-20/FEI Transmission Electron Microscope (TEM). Samples for TEM studies were prepared by ultrasonic dispersing in ethanol and dropping on a copper grid. The surface area was calculated using the BET model. The total pore volume was estimated from the amount of nitrogen adsorbed at P/P_0 = 0.95; the micropore volume was derived from the DR plot; and the pore size distribution (PSD) was calculated based on the density functional theory (DFT). X-Ray photoelectron spectroscopy (XPS) measurements was perfomed using a Kratos Analytical XSAM 800 cpi ESCA equipment equipped with a Mg anode (Mg Kα radiation, 1253.6 eV) and spherical analyzer operating at 15 kV and 15 mA.

Catalytical tests

The experiments of extraction/oxidative desulphurization were conducted in a 20 mL round-bottom flask. For the catalytic studies, 500 mL of a solution containing 1000 mg L^{-1} of dibenzothiophene (DBT) (model compound of a fuel) dissolved in n-hexane was prepared. Of this solution, 10 mL was used to prepare the mixture with acetonitrile (extraction liquid) and the catalyst. The mix, 1 mL H_2O_2 (30 %, v/v) and 2 mL of acetonitrile were stirred vigorously at 25 ^{o}C in the presence of 10 mg of catalyst. After the reaction, the resulting mixture was placed in a static state to form two layers. The upper apolar phase (hexane) was separated quickly from the polar phase (acetonitrile) by decantation and its sulfur content analyzed by gas chromatography. Reuse of the catalyst tests: After 300 min of reaction, the catalysts were recovered by filtration of the modified mixture, followed by washing 3 times to remove the solvents. The materials were then dried in an oven for 12 h at 70 ^{o}C.

The products were analyzed by GC–MS (Agilent). The percentage of dibenzothiophene conversion was quantified by integrating the dibenzothiophene peak to the total ion content obtained before and after the reaction with the catalyst. GC–MS analysis was carried out with an injector temperature of 250 ^{o}C, an injection volume of 0.2 mL and a flow rate of 1.4 mL min^{-1} with an HP-5 column (5 % polymethylphenylsiloxane). Each run used a heating curve of 110^{o}C for 5 min then increasing by 3 ^{o}C min^{-1} to 250 ^{o}C. The concentration in percentage of remaining DBT was monitored using a calibration curve (5 points) constructed with various concentrations of this compound.

The calibration curve was performed in the two solvents, acetonitrile and hexane with an excellent linearity ($R^2 > 0.99$).

Results and discussion

Characterization of the materials

The carbon materials were characterized to better understand the interaction between niobium oxalate and the different carbon supports. Figure 1 shows the Nb3d XPS spectra for the samples niobium oxalate salt, GO-Nb, AC-Nb, and CNT-Nb. The pure niobium oxalate spectrum showed peaks centered at 206.8 ($3d_{5/2}$ core level) and 209.6 eV ($3d_{3/2}$ core level). These signals were slightly shifted in all three types of carbon support due to the interaction between the niobium species and the carbon matrix. Similarly, the XPS spectra for the C1s (Figure 2) and O1s (Figure 3) also indicate the presence of niobium oxalate bound on the carbon materials surface. The C1s spectrum of pure niobium oxalate presented signals at 288.5 and 284.9 eV. The peaks at 287.4, 287.7, and 286.5 eV in the samples AC-Nb, GO-Nb and CNT-Nb suggest the attachment of niobium oxalate on the carbon matrix. The At% calculated is C 33.7%, O 61.6% and Nb 4.7% for niobium oxide, C 67.2%, O 31.6% and Nb 1.2% for GO-Nb, C 84.3%, O 14.0% and Nb 1.7% for AC-Nb and for CNT-Nb is C 92.3%, O 7.4% and Nb 0.3%.For the O1s spectra, it can be seen that the materials without the presence of niobium oxalate present a typical oxygen signal at approximately 532 eV.

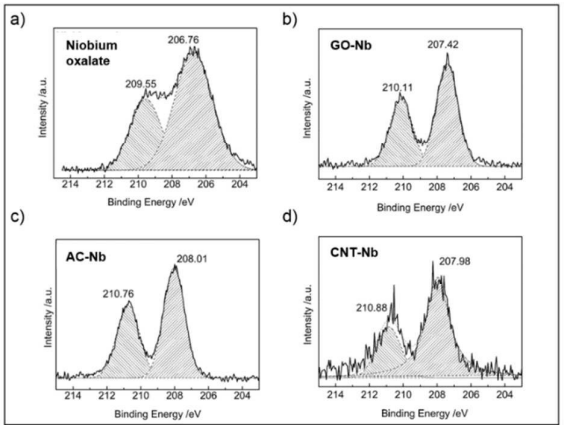

Figure 1 - X-ray photoemission spectra (Nb3d) of (a) pure niobium oxalate, (b) GO-Nb, (c) AC-Nb, and (d) CNT-Nb.

The curve fitting to C1s spectra shows 6 peaks assigned to functional groups in carbonaceous materials [15,16]. Binding energy at 284.4 and 285.3 (±0.2) eV are close to C-C sp2 and sp3 bond hybridization, respectively. The peak at 285.3 eV shows a pronounced shifts for GO and GO-Nb, and for AC and AC-Nb. Binding energy at 286.5 eV (-COH), 297.6 eV (C=O), 288.8 eV (-COOH) and 290.2 eV (-COO) shows the interaction with functional groups, these are modified clearly for GO-Nb and CA-Nb and more subtle for CNT-Nb, showing the presence of niobium oxalate on the materials surface. The curve fitting to O1s spectra show 3 peaks associated with O=C (531.2±0.4 eV), O-C (533.4±0.4 eV) and O-water (534.6±0.3 eV) bonds.However, because of the bond between niobium oxalate and the carbon materials a more intense signal at 536 eV can be observed. These signals are indicative of the presence of niobium oxalate embedded into the carbon, showing

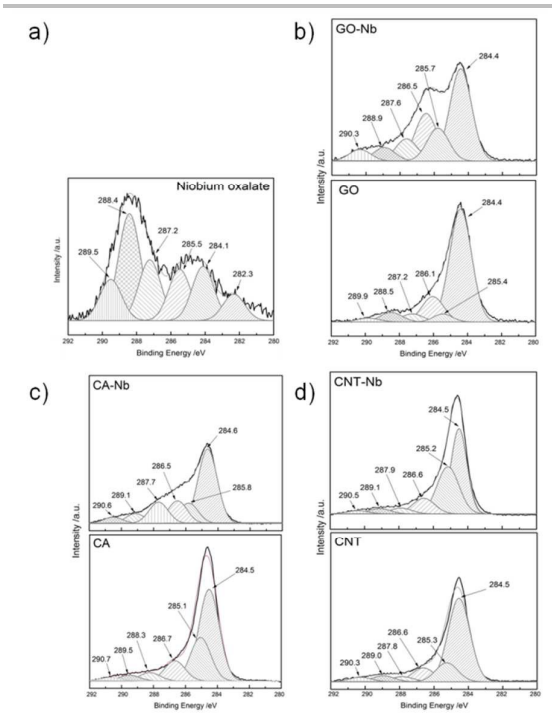

Figure 2 - X-ray photoemission spectra (C1s) of (a) pure niobium oxalate, (b) GO-Nb, (c) AC-Nb and (d) CNT-Nb.

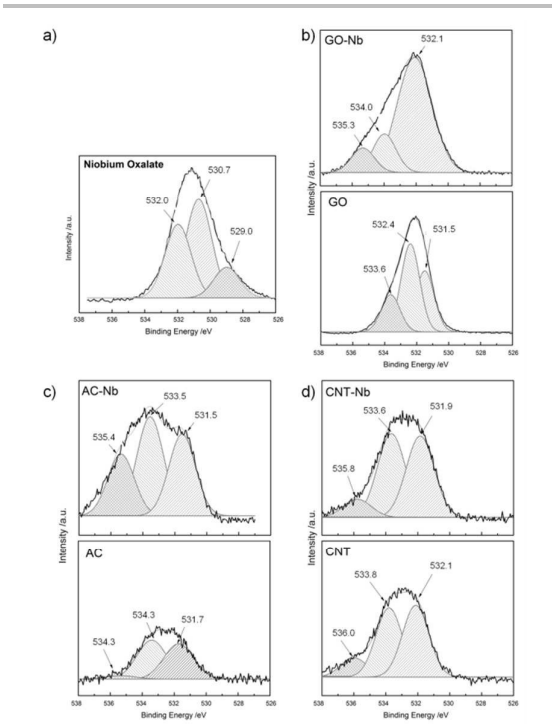

Figure 3 - X-ray photoemission spectra (O1s) of (a) pure niobium oxalate, (b) GO-Nb and GO, (c) AC-Nb and AC, and (d) CNT-Nb and CNT.

that niobium is present in the form of niobium oxalate without formation of niobium oxide, as widely reported in literature [17]. Therefore, niobium is highly dispersed on the surface of the

carbonaceous materials in the form of single sites, making them promising materials for catalytic reactions where the niobium acts as the active phase.

In order to confirm that the niobium compound has been immobilized unaltered on the carbon surfaces (graphene oxide) IR analyses were performed (Figure 4). Considering the pure oxalate niobium spectrum, peaks can be observed at 1734 and 1680 cm^{-1} relating to vibration of the C = O bond. Furthermore, at 1390 cm^{-1} there is a signal related to the CO vibration. After the incorporation of niobium oxalate in graphene oxide such signs can be observed in the GO-Nb material, but with a slight shift indicating binding to the surface of the carbonaceous material. It is interestingly to observe that pure graphene (GO) showed no signals in this spectral region.

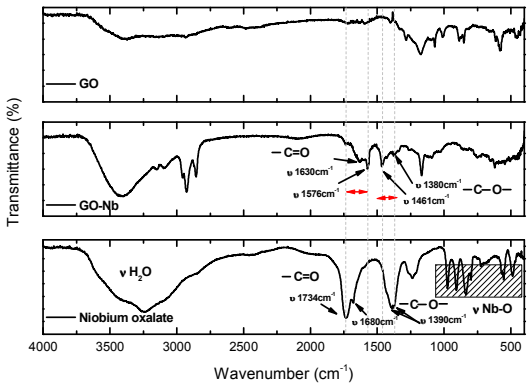

Figure 4 – IR analysis to show niobium compound on the carbon surface (graphen oxide)

Raman spectroscopy was used to investigate the interfacial interaction between the niobium oxalate and carbon matrixes (Figure 5).

Two characteristic peaks due to the D band (amorphous/disordered sp^3 carbon) and G band (graphitic sp^2 carbon) were observed in the spectra of all samples. The intensity ratios of these bands (I_D/I_G) were 1.92 and 0.96 for the samples CNT-Nb and CNT, respectively. For the samples AC-Nb and AC, the I_D/I_G ratios were 1.21 and 1.02 and for GO-Nb and GO these ratios were 1.24 and 0.55, respectively. An increase of the I_D/I_G ratio for GO of 0.55 to 1.12, is probably due to an additional exfoliation of the material during the ultrasound and reflux treatments. The change in the I_D/I_G ratio with exfoliation has been reported in the literature [18]. However, this ratio is even greater, 1.24, in the presence of the niobium salt. These findings suggest that the incorporation of niobium oxalate caused an increasing in the amounts of defects on the carbon matrixes. It is a strong evidence that niobium oxalate is bonded on the carbon supports.

Images obtained by TEM (Figures 6-8) show typical morphologies of the carbonaceous materials. For all samples, particles that could be assigned to the precipitation of the Nb precursor or formation of niobium oxides (since the temperature of the system during the synthesis procedure did not exceed 100 °C) were not clearly observed. However considering the EDS data (Figure 6-8c), collected in different regions of the samples, the presence of niobium element is imperative. Therefore, this is an indicative of the formation of niobium complexes as isolated sites on the carbon materials surface. In fact, in works described in the literature related to deposition of niobium oxide on the surface of carbonaceous materials, the niobium particles are well distinguishable from the carbon matrix [19]. Li and coworkers prepared Nb_2O_5 nanorods distributed on the graphite felts (GFs) using a hydrothermal method (T = 443 K) with ammonium niobium oxalate as Nb precursor [19]. White solid precipitates were observed in the autoclave and on the surfaces of the GFs after the synthesis. These researchers found, by field emission scanning electron microscopy, nanoparticles on the surface of GFs, in which the amount varied as a function of the concentration of Nb in the precursor solutions.

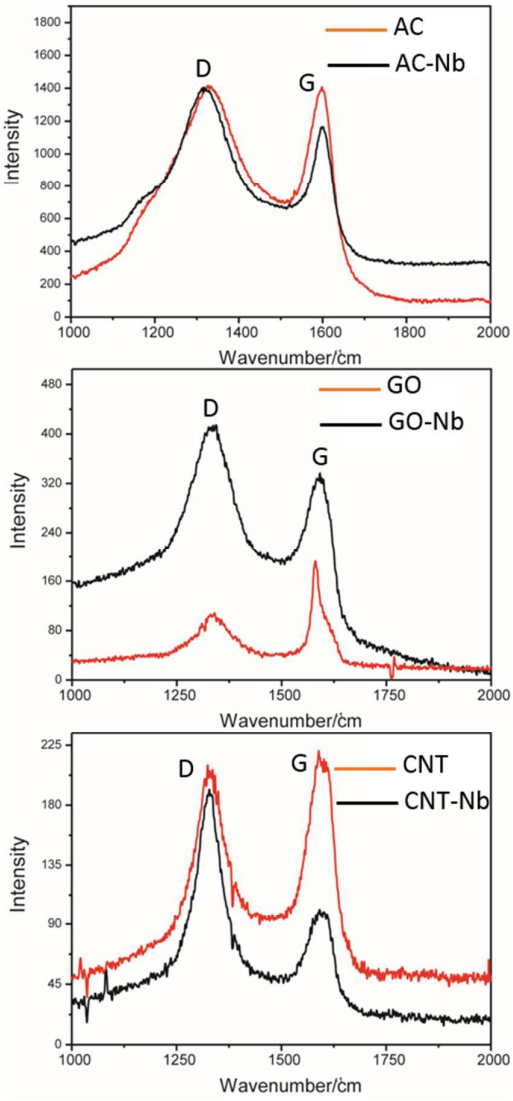

Figure 5 -Raman spectra of the investigated catalysts.

The attachment of niobium oxalate influences the thermal behavior of the all carbon supports, as can be seen in Figure 6d for the CNT-Nb sample for GO-Nb (Figure 7) and AC-Nb (Figure

8). The maxima of the DTG curve shift to lower values, decreasing about 20 °C for the CNT-Nb and 40 °C for activated carbon (AC-Nb). Interestingly, for the graphene oxide modified with niobium (GO-Nb) there is an increase of about 40 °C in

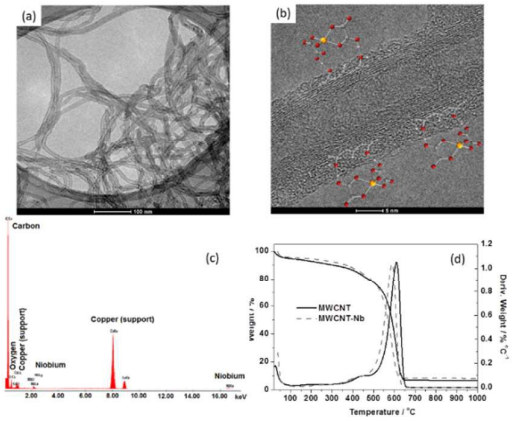

Figure 6 - (a,b) TEM images of oxidized MWCNT modified with niobium oxalate (CNT-Nb). Scale bars in (a): 100nm and (b): 5nm. (c) CNT-Nb EDS data and (d) TG and DTG curves for oxidizedCNT and CNT-Nb.

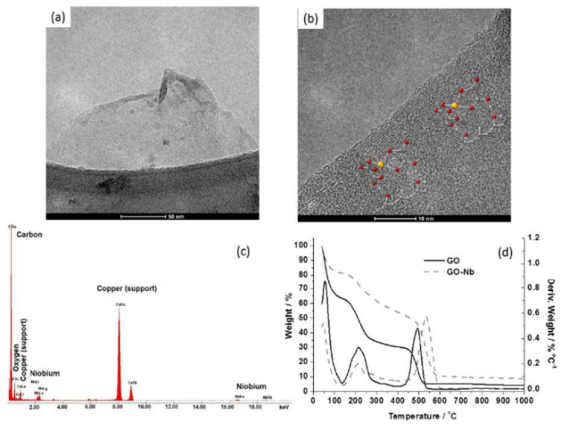

Figure 7 - (a,b) TEM images of few-layer graphene oxide modified with niobium oxalate (GO-Nb). Scale bars in (a): 50nm and (b): 10nm. (c) GO-Nb EDS data and (d) TG and DTG curves for few layer graphene oxide (GO) and GO-Nb.

the DTG maximum.

From TG data, it could be verified that the presence of niobium increases the thermal stability of the GO-Nb material. There is not a clear explanation for this effect. Probably this is the material with the higher amount of Nb because it has about

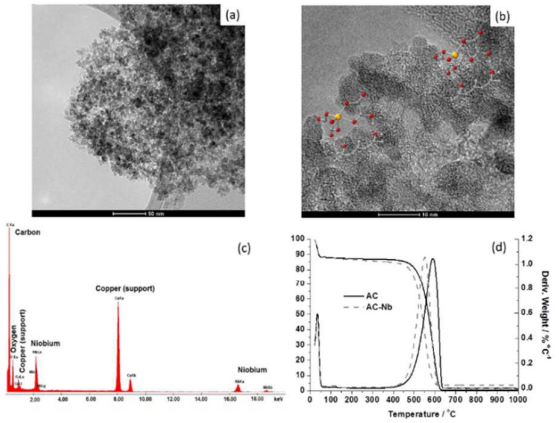

Figure 8 -(a,b) TEM images of activated carbon modified with niobium oxalate (AC-Nb). Scale bars in (a): 50nm and (b): 10nm. (c) AC-Nb EDS data and (d) TG and DTG curves for activated carbon (AC) and AC-Nb.

30% of oxygenated groups on its surface, which exert influence on the thermal degradation process. The changes in the weight losses related to decomposition of the carbon structures are more pronounced for the activated carbon and graphene oxide. In all samples, there is an increase in the amount of residue at 1000 °C, probably related to the formation of niobium oxide after the heating in an oxidizing atmosphere. The results via thermogravimetry analyses indicate that the GO-Nb showed higher Nb content, and the amounts for the three materials were 0.6, 1.1 and 1.6% for the CNT-Nb catalysts, AC-Nb and GO-Nb, respectively.

Catalytic tests

Several studies of DBT oxidation have been developed because it is a pollutant responsible for sulfide contamination in petroleum, and the removal of this pollutant has been investigated in biphasic reactions [20]. The increasing in the DBT polarity makes it migrates to polar solvent, which can be separated by liquid-liquid extraction. The Nb-containing carbon materials were tested for DBT oxidation to verify their catalytic properties. The DBT oxidation in a biphasic system (hexane/acetonitrile) was studied as a reaction test (Figure 9). In our tests, the single sites of niobium oxalate on the surface of carbonaceous material (activated carbon, carbon nanotube and graphene oxide) were responsible for the activation of H_2O_2, generating highly reactive sites called peroxo groups [21-26], which oxidize DBT generating the corresponding sulfone

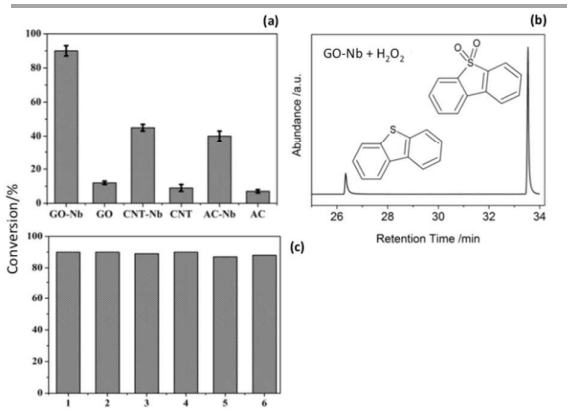

Figure 9 -Conversion of DBT using Nb-modified carbonaceous materials (a). Chromatograms of the DBT removal (a) in the presence of GO-Nb and extracted sulfone washed with H_2O after the reaction (b). Reuses tests using GO-Nb catalyst (c). Reaction conditions: mass of catalyst = 10 mg; 0.1 mL of H_2O_2 (35 %); reaction time = 30 min.

groups.

The GO-Nb catalyst presented a high efficiency to remove DBT with about 90% of conversion. On the other hand, without the niobium it was observed a removal of approximately 12 %, probably due to adsorption process and also hydrogen peroxide action. In our tests we found that the sulfone generated by the oxidation of DBT did not migrate to the polar solvent as related in other works using other catalyst types [20], but carbonaceous material totally adsorbed it.

Indeed, the formation of the sulfone was detected only after the recovery of carbonaceous material and washing with H_2O for extraction of sulfone adsorbed on activated carbon, carbon nanotube or graphene oxide as displayed in the chromatogram in Figure 9 (showed for GO-Nb).

It can be observed a low intensity signal related to DBT and a strong sulfone signal obtained by extraction with H_2O from the catalyst after reactions. Similar results were found for the AC-Nb and CNT-Nb catalysts. We believe that the presence of oxygen groups after niobium complex incorporation over carbons matrix increase the polar properties of the surface, making them good adsorbents for oxidized pollutants. This result shows that the modified niobium oxalate material can be used both as a catalyst and adsorbent of the oxidized fraction of the pollutant, avoiding the need to use an extraction solvent, which makes the process more environmentally friendly. Figure 9c shows the reuses tests. The reuse of the GO-Nb catalyst was tested in six subsequent reactions. The conversion remained constant at approximately 90%, indicating the high stability of the Nb-modified grapheme oxide. To check a possible leaching of niobium oxalate as well as reaction via homogeneous process the GO-Nb catalyst was placed in acetonitrile and stirred for 60 min. The catalyst was then removed by centrifugation and a solution of DBT in hexane was added to the system. After 60 min of reaction, oxidation products of DBT were not detected.In summary, the presence of niobium in the material appears to direct a greater catalytic activity, since the modified graphene with niobium complex showed higher capacity of the DBT conversion.

Theoretical calculations

All theoretical calculations were performed using the Gaussian 09 program package [27]. The gas-phase structures were optimized with PBE [28] exchange-correlation functional and 6-311++G(d,p) for all atoms except for niobium for which we have used the SDDALL basis set. Harmonic frequencies were evaluated to confirm that the analyzed structures are true minima in the potential energy surface (PES). For all structures, the non-specific solvent effect was assessed using the united atoms Hartree-Fock/polarizable continuum model (UAHF/PCM)[29-30]. In this approach, the solute is immersed in a polarizable cavity that is formed by spheres centered on atomic groups. This model considers that inside the cavity the dielectric constant is the same as in vacuum while the dielectric constant outside the cavity was found the same as acetonitrile (ε= 35.688). The optimized structures obtained in the gas phase calculations were used to estimate the solvent effect through single point calculations at the HF/6-31+G(d,p) level of theory. It is worth mentioning that the combination of DFT optimization procedures and single point PCM calculations have already been employed with success in several complex systems[31-32]. For all the possible adsorption processes studied the total Gibbs free energy was evaluated according Equation 1.

$$\Delta G^{total} = \Delta E^{ele} + \Delta G^{therm} + \Delta\Delta G^{solv} \quad (1)$$

Where ΔE^{ele} is related to the reaction energies, ΔG^{therm} is the thermal correction for Gibbs free energies and $\Delta\Delta G^{solv}$ is the solvation energies.

We have started the analysis with the chemical speciation of the oxalate niobium complex. Experimental data from X-ray diffraction show that this complex is a heptacoordinated species [33, 34], presenting two water molecules in its coordination sphere. Figure 10(a) shows a schematic representation of the proposed water molecule withdrawal process. In the first species, one can note that there are two distinct water molecules in the complex, in axial and equatorial positions. The total Gibbs free energy (including the solvent effect) related to the first water molecule is about -4.2 and -3.0 kcal mol^{-1} for the delivery of the axial and equatorial water molecules, respectively. The release of the two water molecules gives rise to the $[Nb(O)(ox)_2]^-$ that was used to interact with the activated carbon.

Another possible species that can interact with the activated

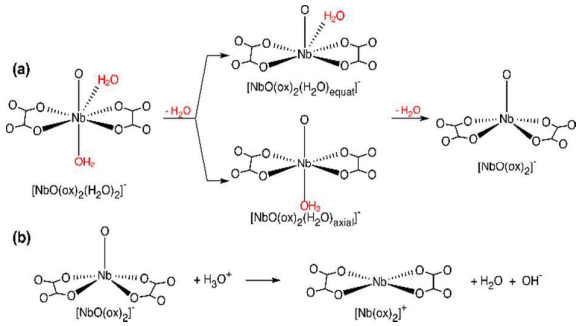

Figure 10 - Representative scheme of the chemical speciation of the (a) heptacoordinated niobium species and (b) removal process of the oxo group from the $[NbO(ox)_2]^-$ species.

carbon is that originated from the elimination of the oxo group (Figure 10(b)), the $[Nb(ox)_2]^+$ species. This process is highly endergonic with total Gibbs free energy equal to +122.2 kcal mol^{-1}. In some adsorption models, this species was used to interact with the activated carbon, and this endergonic formation process was taken into account.

The model adopted for the simulation of the activated carbon was a small graphene-like sheet of carbon atoms saturated in the borders with hydrogen atoms. In this model we have used 32 carbon atoms to simulate the graphene sheet. Different substitutions have been made in this model in order to include oxo, carboxylate, carboxylic and hydroxyl groups functionalizing the graphene. The distinct models used can be viewed in Figure S1 in the Supplementary Information (SI). As can be observed in Figure S1 many adsorption models have been investigated, and Table S1 displays the thermodynamic properties of all studied models. According to the energetics contained in Table S1 the most favorable adsorption model (Reaction I) is an ionic association between the $[NbO(ox)_2]^-$ and a substituted graphene with two protonated hydroxyl groups (Figure 11). The Gibbs free energy associated with this adsorption model is -108.7 kcal mol^{-1}, showing to be a spontaneous process. This activated carbon model is reasonable since the reaction medium is highly acidic, and the

protonation of hydroxyl groups on the surface is possible. This adsorbed species is interesting because the niobium atom in its structure is accessible to a coordinative unsaturated site. Another important fact that gives support for this model is related to the Mülliken charge on the niobium atom that in the $[NbO(ox)_2]^-$ species is +1.02 and increases to +1.07 in the adsorbed complex, what can make easier the coordenation of DBT in the catalyst.

All studied interaction complexes can occur at the reactional conditions and one of them considers the change in the carbon atom environment (Figure 12). In this model, the Nb complex reacts with some C*sp*2 of the intact graphene structure and a new bond between these C atoms and some parts of the Nb complex are created, giving rise to a new C*sp*3 atom in the graphene sheet, with the Nb complex being covalently attached at the end, which is in agreement with the Raman spectra.

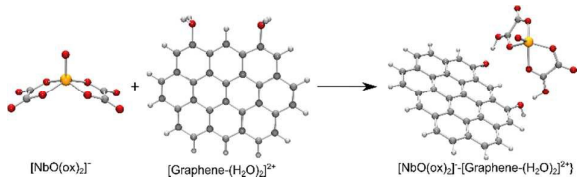

Figure 11 - Most favorable process of the $[NbO(ox)2]^-$ species on the hydroxylated graphene model.

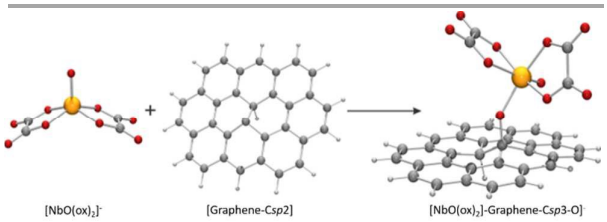

Figure 12 – Simulated model for the interaction of oxo bis oxalate niobate(V) coordinated to an oxygen atom bounded to a sp^3 carbon.

Conclusions

We showed for the first time an effective way for incorporation of active niobium species on the surface of carbonaceous materials. Thermogravimetric analysis indicated the presence of different amounts of niobium species over carbonaceous materials. This result allowed quantifying the Nb content present in those different materials. XPS analysis also indicated the presence of niobium species with peak at about 531 eV. The GO-Nb catalyst showed high capacity of sulfur compounds oxidation. Catalytic tests with dibenzothiophene (DBT) showed capacity removal of approximately 90% from the apolar part in a biphasic mixture using GO-Nb catalyst. Interestingly, the materials showed versatility, since after the oxidation of DBT to sulfone, as identified by GCMS, occurs adsorption at the surface of the carbonaceous material.

Acknowledgements

Financial support from the Fapemig, CNPq and Pro-reitoria de pesquisa-UFMG.

References

1 S. Castro, M.C. Guerreiro, L.C.A. Oliveira, M. Gonçalves, A.S. Anastácio, M. Nazzarro, *Applied Catalysis A: General*, 2009, **367,** 53.
2 L.C.A. Oliveira, M.C. Guerreiro, M. Gonçalves, D.Q.L. Oliveira, L.C.M. Costa, *Materials Letters*, 2008, **62,** 3710.
3 C. Huang, C. Li, G. Shi, *Energy and Environmental Science*, 2012, **5,** 8848.
4 G. Blanita, M.D. Lazar, *Micro and Nanosystems*, 2013, **5,** 138.
5 L.M. Ombaka, P. Ndungu, V.O. Nyamori, *Catalysis Today*, 2013, **217**, 65.
6 G. M. Scheuermann, L. Rumi, P. Steurer, W. Bannwarth, R. Mülhaupt, *J. Am. Chem. Soc.,* 2009, **131**, 8262.
7 X. Zhou, J. Qiao, L. Yang, J. Zhang, *Adv. Energy Mat,* 2014, 1301523.
8 L. Shang, T. Bian, B. Zhang, D. Zhang, L. Z. Wu, C. H. Tung, Y. Yin, T. Zhang, *Angew. Chem.,* 2013, **53**, 250.
9 A. Kongkanand, K. Vinodgopal, S. Kuwabata, P. V. Kamat, *J. Phys. Chem. B,* 2006, **110**, 16185.
10 X. Chen, G. Wu, J. Chen, X. Chen, Z. Xie, X. Wang, *J. Am. Chem Soc,* 2011, **133**, 3693.
11 P. V. Kamat, *J. Phys. Chem. Lett,* 2010, **1**, 520.
12 Y. Okamoto, K. Fukino, T. Imanaka, S. Teranishi, *Journal of Catalysis*, 1982, **74**, 173.
13 X. Zhang, J. Guo, P. Guan, C. Liu, H. Huang, F. Xue, X. Dong, S.J. Pennycook, M.F. Chisholm, *Nature communications*, 2013, **4**, 1924.
14 D.C. Marcano, D.V. Kosynkin, J.M. Berlin, A. Sinitskii, Z. Sun, A. Slesarev, L.B. Alemany, W. Lu, J.M. Tour, *ACS Nano*, 2010, **4,** 4806.
15 R. Larciprete, S. Gardonio, L. Petaccia, L. Lizzit, *Carbon*, 2009, **47**, 2579.
16 L. Chen, Z. Chu, J. Li, B. Zhou, M. Shan, Y. Li, L. Liu, B. Li, J. Niu, *RSC Adv.,* 2014, **4**, 1025.
17 R.K. Sharma, A. Pandey, S. Gulati, *Applied Catalysis A: General*, 2012, **431–432**, 33.
18 C. Botas, A. M. Pérez-Mas, P. Álvarez, R. Santamaría, M. Granda, C. Blanco, R. Menendéz, *Carbon*, 2013, **63**, 562.
19 B. Li, M. Gu, Z. Nie, X. Wei, C. Wang, V. Sprenkle, W. Wang, *Nano Letters*, 2013, **14**, 158.
20 L.C.A. de Oliveira, N.T. Costa, J.R. Pliego Jr, A.C. Silva, P.P. de Souza, P.S. de O. Patrício, *Applied Catalysis B: Environmental*, 2014, **147,** 43.
21 F. G. E. Nogueira, J. H. Lopes, A. C. Silva, M. Gonçalves, A. S. Anastácio, K. Sapag, L. C. A. Oliveira, *Applied Clay Science,* 2009, **43**, 190.

22 P. Chagas, H.S. Oliveira, R. Mambrini, M. Le Hyaric, M.V. de Almeida, L.C.A. Oliveira, *Applied Catalysis A: General*, 2013, **454**, 88.
23 L.C.A. Oliveira, M.F. Portilho, A.C. Silva, H.A. Taroco, P.P. Souza, *Applied Catalysis B: Environmental*, 2012, **117–118**, 29.
24 I. S. X. Pinto, P. H. V. V. Pacheco, J. V. Coelho, E. Lorençon, J. D. Ardisson, J. D. Fabris, P. P. de Souza, K. W. H. Krambrock, L. C. A. Oliveira, M. C. Pereira, *Applied Catalysis B: Enviromental,* 2012, **119-120**, 175.
25 W.F. de Souza, I.R. Guimaraes, M.C. Guerreiro, L.C.A. Oliveira, *Applied Catalysis A-Geneneral*, 2009, **360**, 205.
26 C.S. Castro, L.C.A. Oliveira, M.C. Guerreiro, *Catalysis Letters*, 2009, **133,** 41.
27 M.J.T. Frisch, G. W.; Schlegel, H. B.; Scuseria, G. E.; Robb, M. A.; Cheeseman, J. R.; Montgomery, Jr., J. A.; Vreven, T.; Kudin, K. N.; Burant, J. C.; Millam, J. M.; Iyengar, S. S.; Tomasi, J.; Barone, V.; Mennucci, B.; Cossi, M.; Scalmani, G.; Rega, N.; Petersson, G. A.; Nakatsuji, H.; Hada, M.; Ehara, M.; Toyota, K.; Fukuda, R.; Hasegawa, J.; Ishida, M.; Nakajima, T.; Honda, Y.; Kitao, O.; Nakai, H.; Klene, M.; Li, X.; Knox, J. E.; Hratchian, H. P.; Cross, J. B.; Bakken, V.; Adamo, C.; Jaramillo, J.; Gomperts, R.; Stratmann, R. E.; Yazyev, O.; Austin, A. J.; Cammi, R.; Pomelli, C.; Ochterski, J. W.; Ayala, P. Y.; Morokuma, K.; Voth, G. A.; Salvador, P.; Dannenberg, J. J.; Zakrzewski, V. G.; Dapprich, S.; Daniels, A. D.; Strain, M. C.; Farkas, O.; Malick, D. K.; Rabuck, A. D.; Raghavachari, K.; Foresman, J. B.; Ortiz, J. V.; Cui, Q.; Baboul, A. G.; Clifford, S.; Cioslowski, J.; Stefanov, B. B.; Liu, G.; Liashenko, A.; Piskorz, P.; Komaromi, I.; Martin, R. L.; Fox, D. J.; Keith, T.; Al-Laham, M. A.; Peng, C. Y.; Nanayakkara, A.; Challacombe, M.; Gill, P. M. W.; Johnson, B.; Chen, W.; Wong, M. W.; Gonzalez, C.; and Pople, J. A., Gaussian 03, in, Gaussian, Inc., Wallingford, USA, 2004.
28 J.P. Perdew, K. Burke, M. Ernzerhof, *Physical Review Letters*, 1996, **77**, 3865.
29 M. Cossi, V. Barone, R. Cammi, J. Tomasi, *Chemistry Physics Letters,* 1996, **255**, 327.
30 J. Tomase, M. Persico, *Chemical Reviews,* 1994, **94**,2027.
31 H. A. de Abreu, L. Guimarães, H. A. Duarte, *International Journal of Quantum Chemistry,* 2008, **108,** 2467.
32 L. Guimarães, H. A. De Abreu, H. A. Duarte, *Chemical Physics,* 2007, **333,** 10.
33 N.B. Galešić, N., B. Matković, M. Herceg, B. Zelenko, M. Šljukić, B. Prelesnik, R. Herak, *Journal of the Less Common Metals*, 1977, **51**, 259.
34 L.S. Eriksson, G.; Tabachenko, V., *Acta Chemica Scandinavica*, 1993, **47,** 1038.